Actividad solar y estelar

Juan Fabregat

Observatorio Astronómico de la Universidad de Valencia

Catálogo de fuentes de HEAO-1

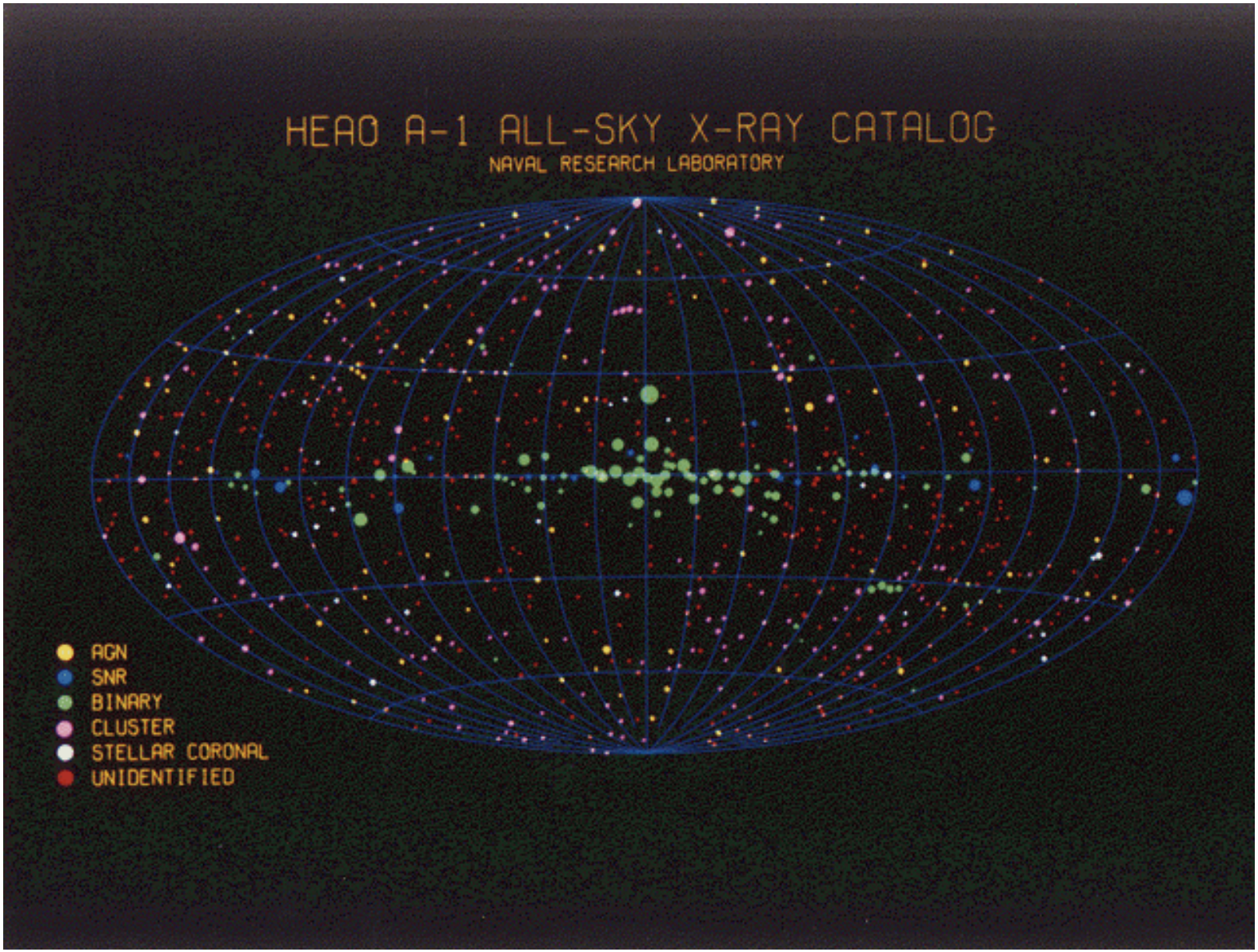

La corona solar en rayos X

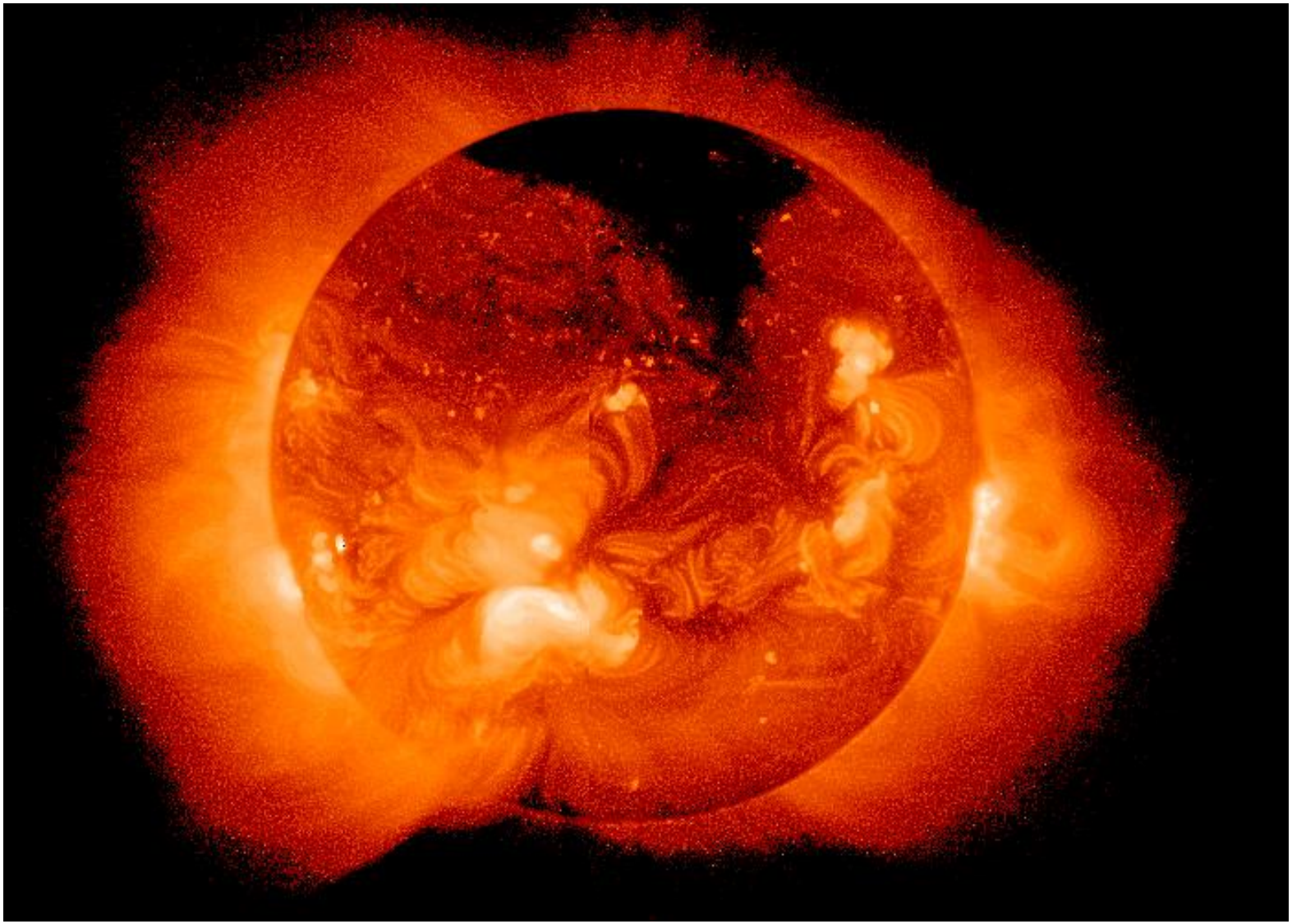

Temperatura en la atmósfera solar

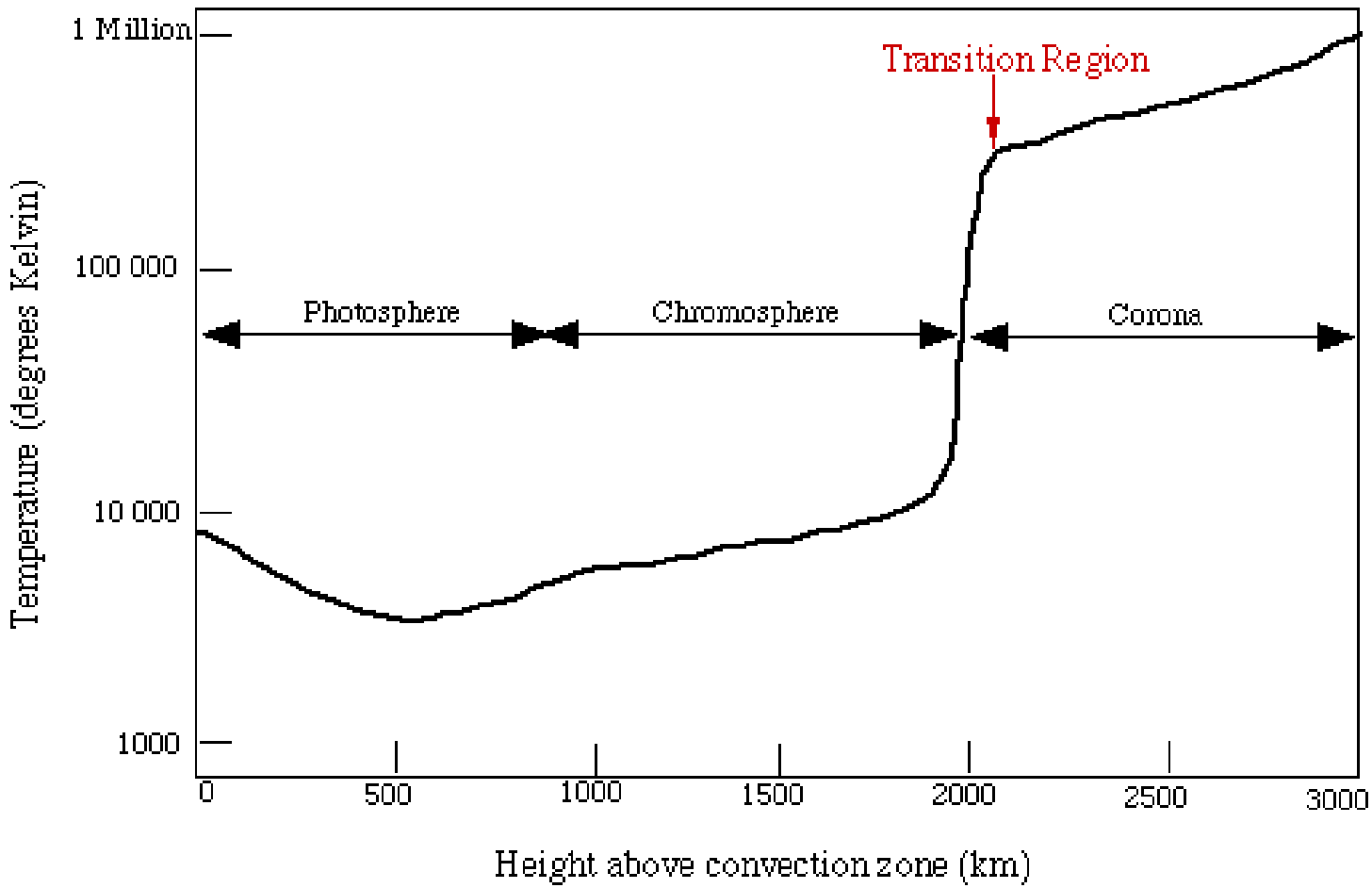

Estructura del Sol

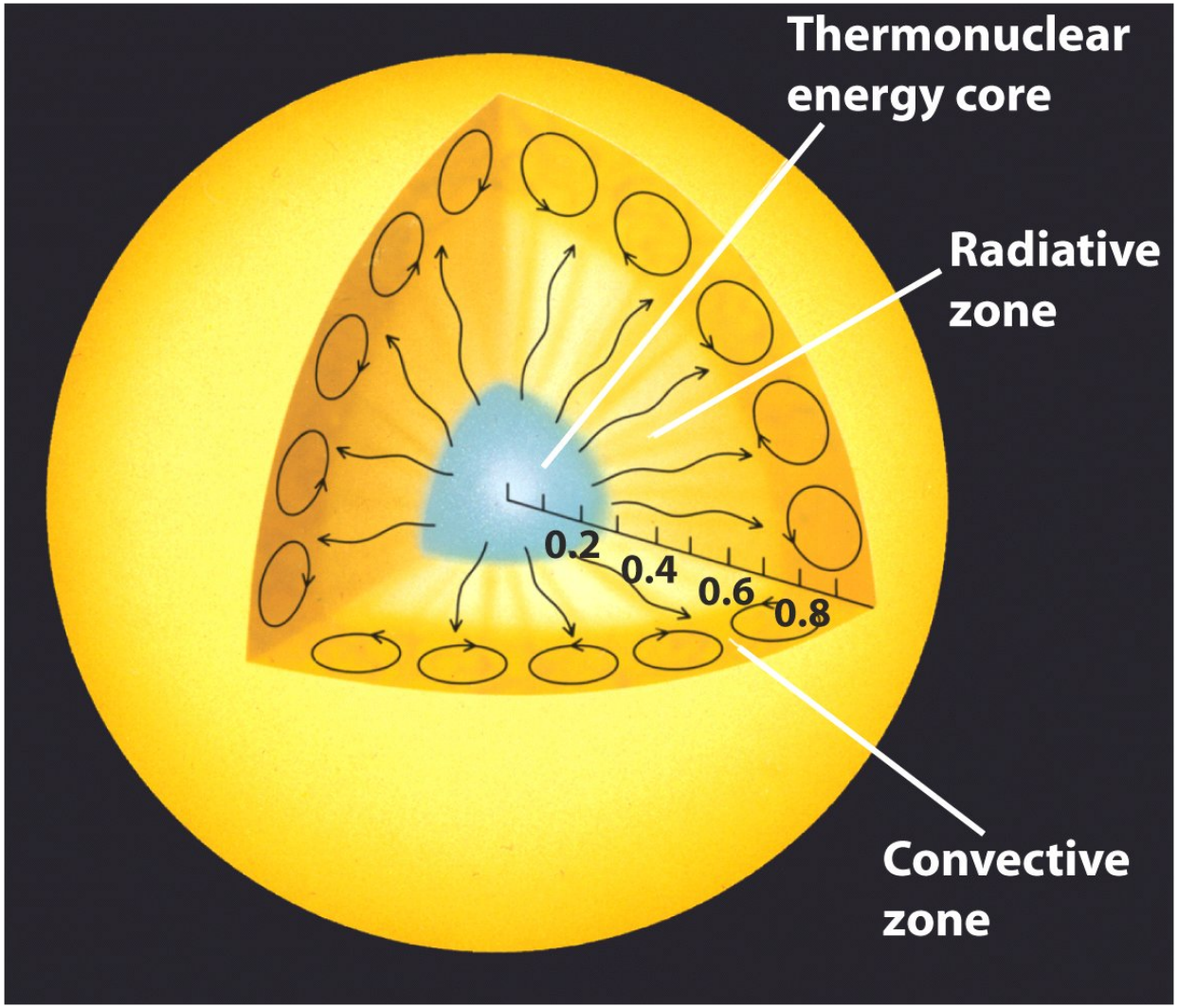

Granulación

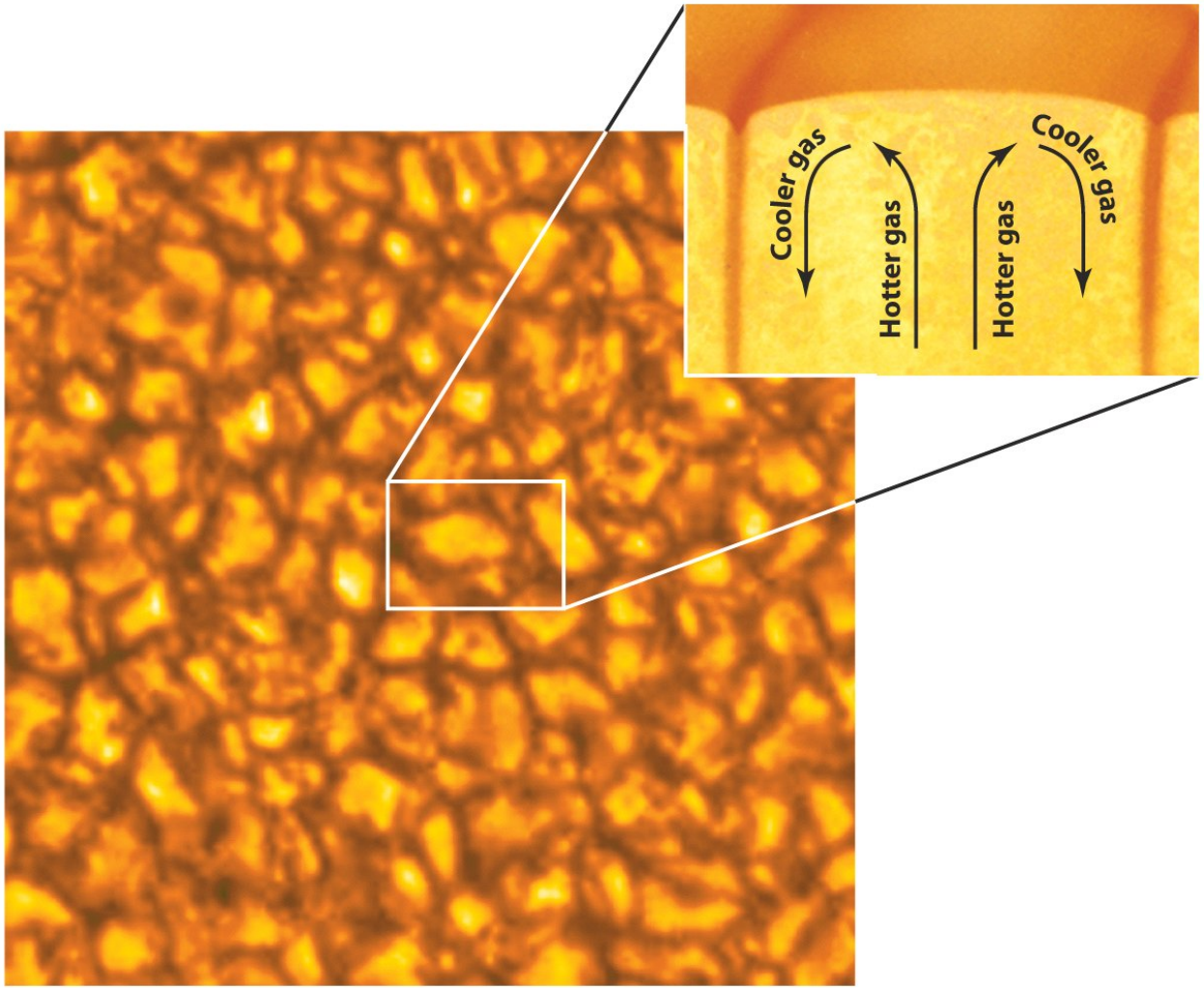

Flotabilidad magnética

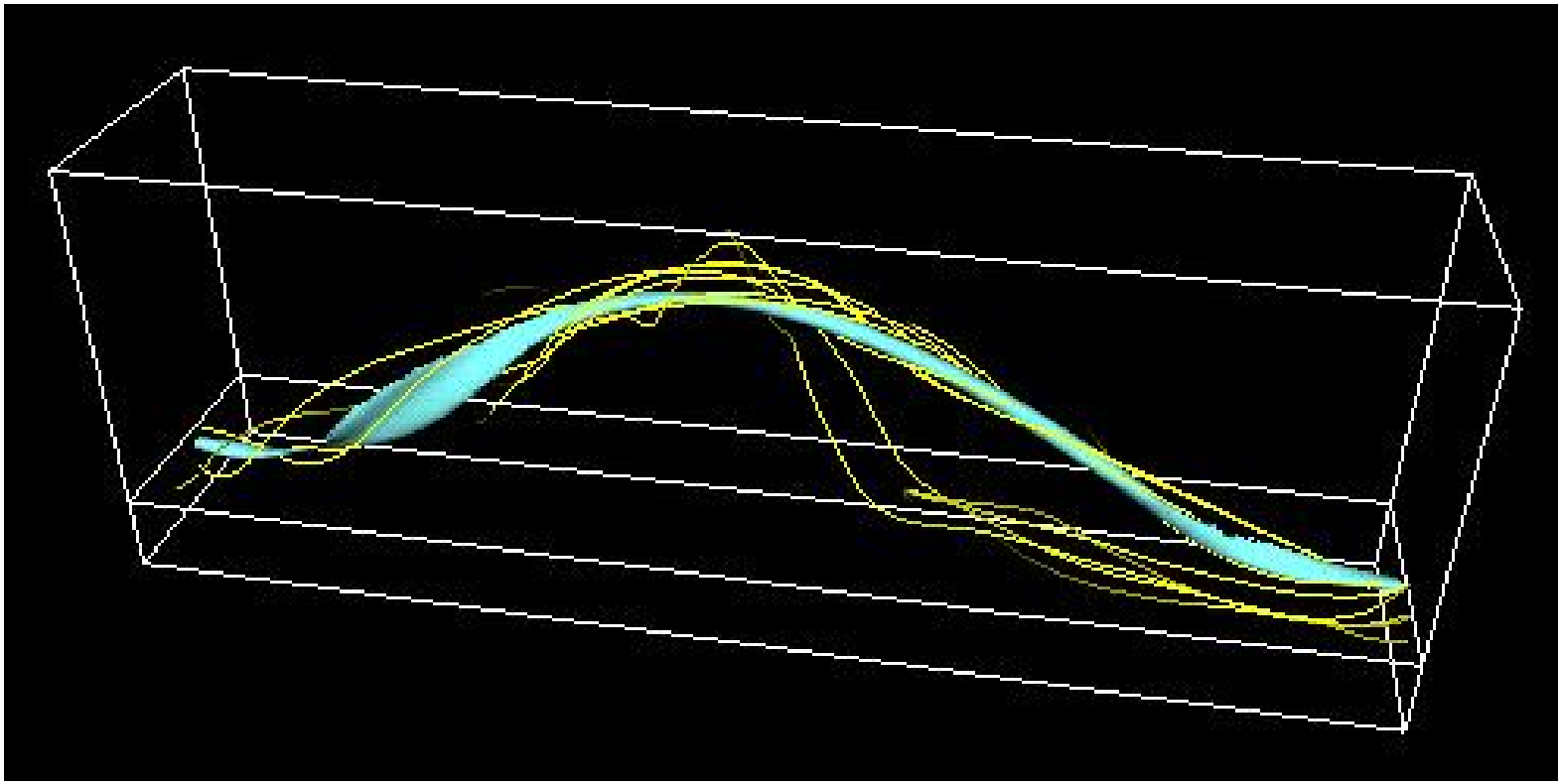

Flotabilidad magnética

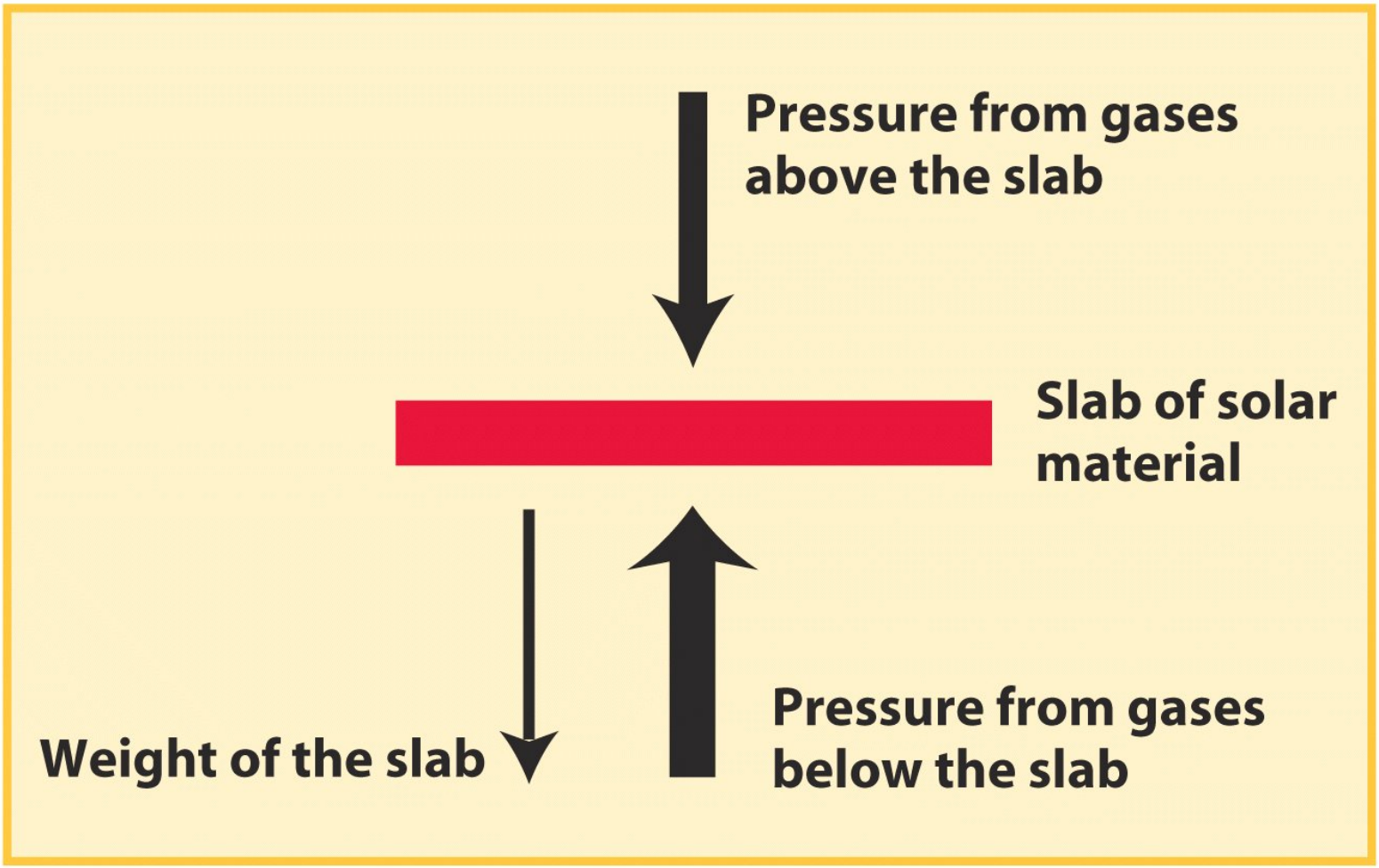

Material inside the sun is in hydrostatic equilibrium, so forces balance

Corona solar

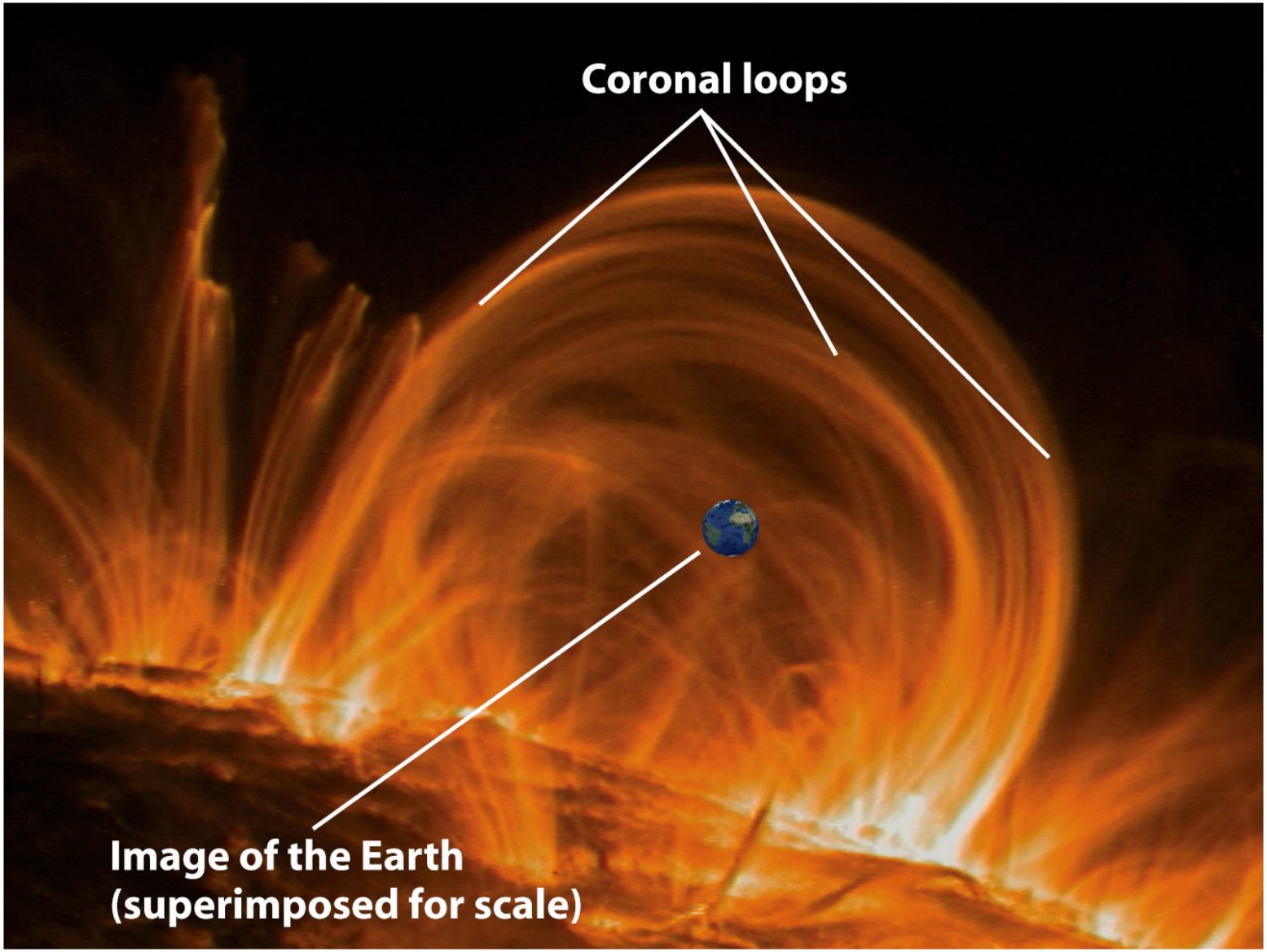

Manchas solares

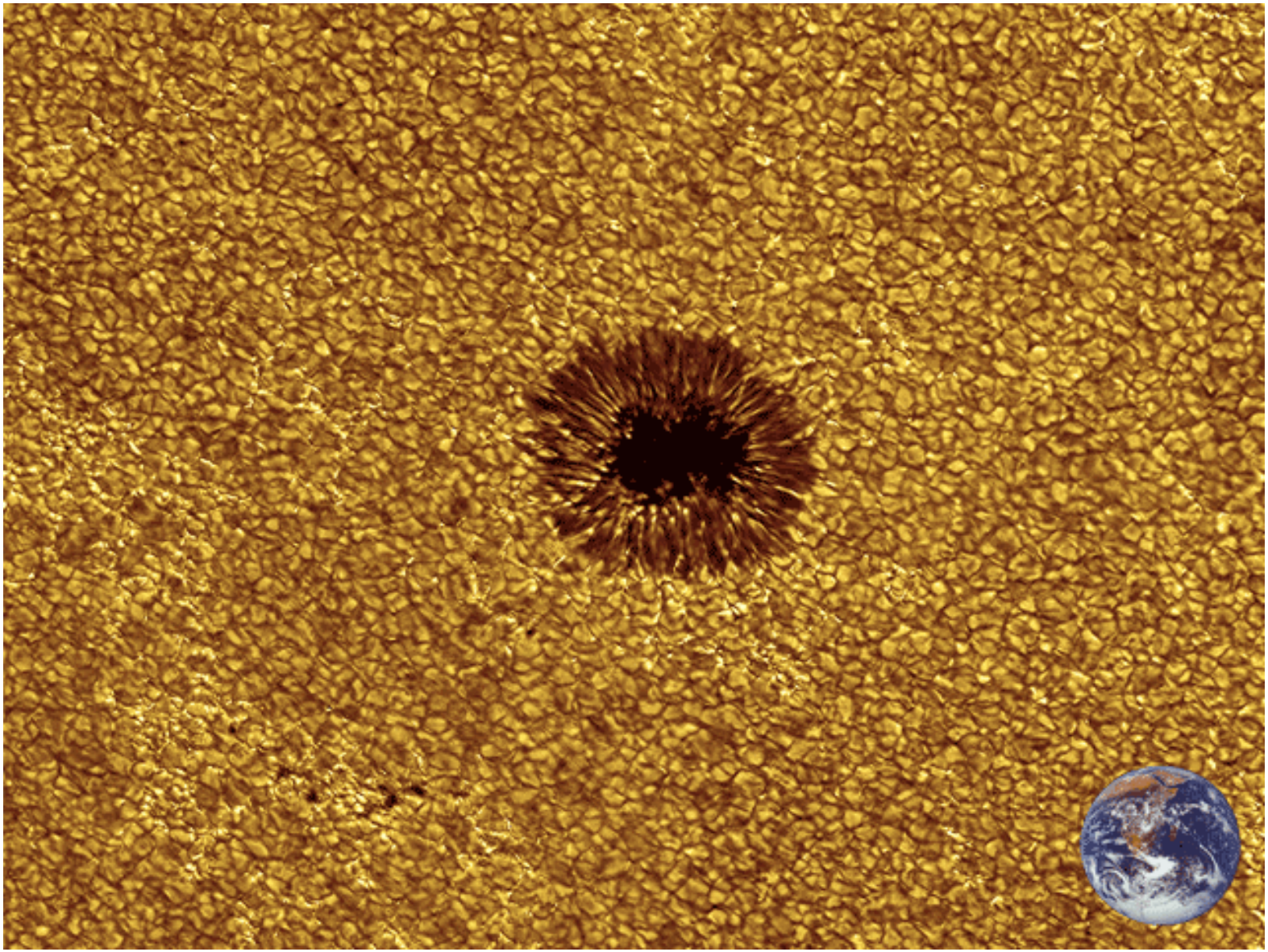

Manchas solares

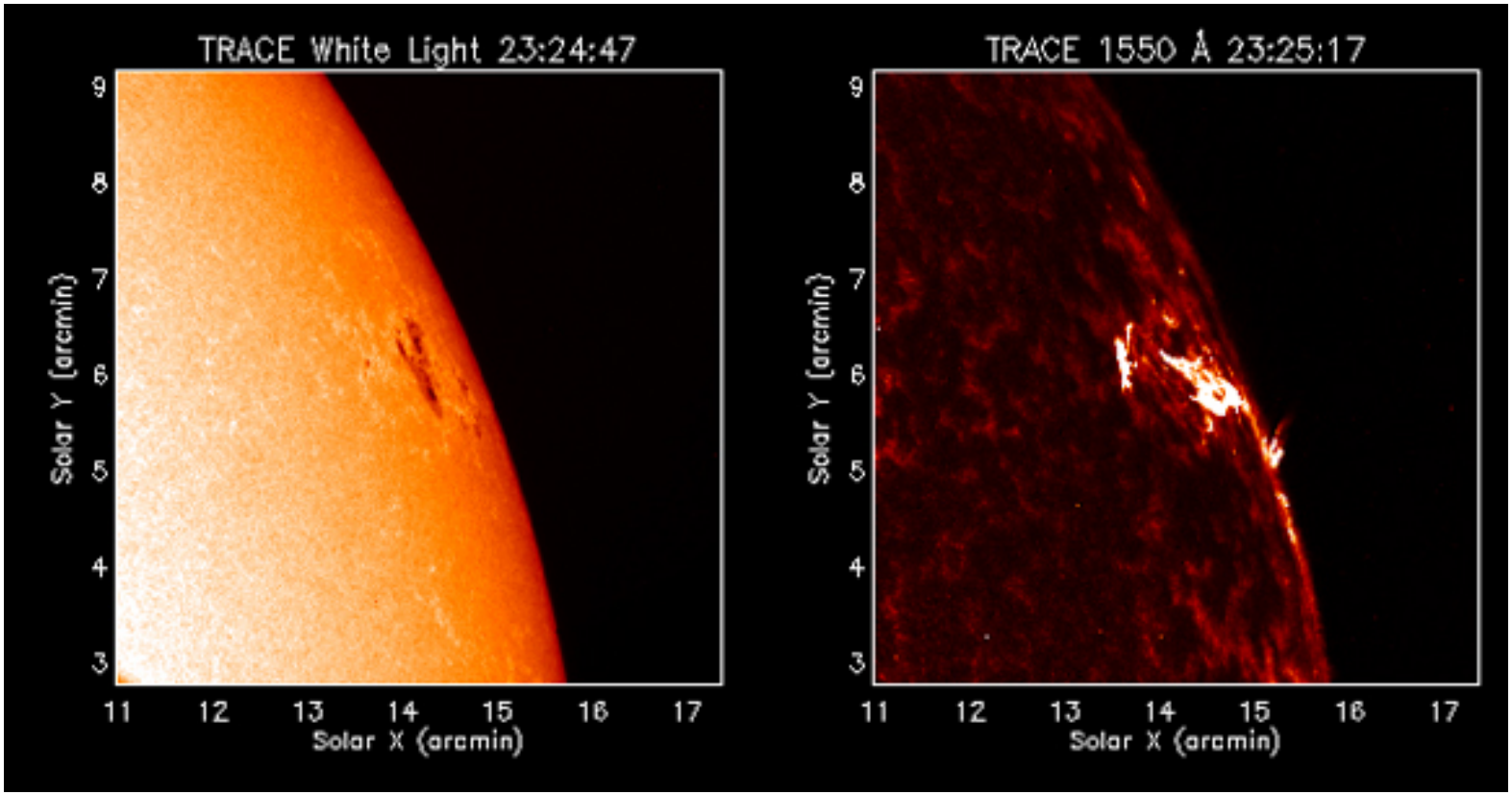

Manchas solares

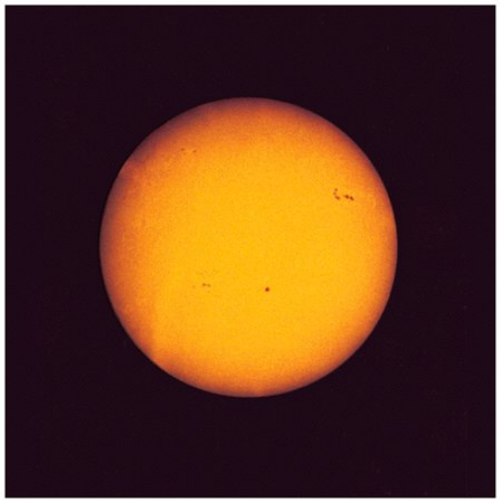

(a) Visible-light image

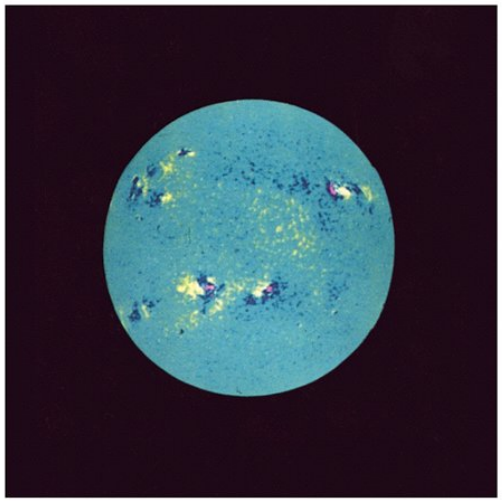

(b) Magnetogram

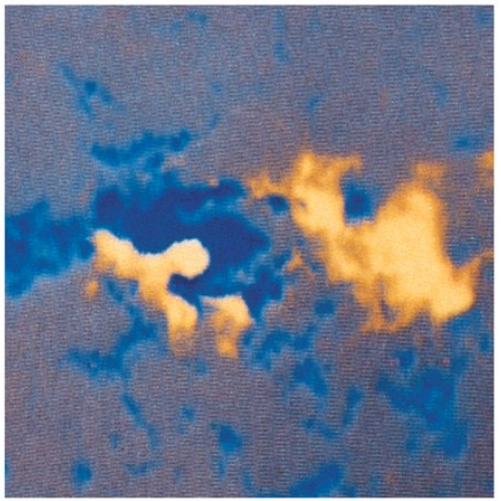

(c) Magnetogram of a sunspot group

Bucle magnético

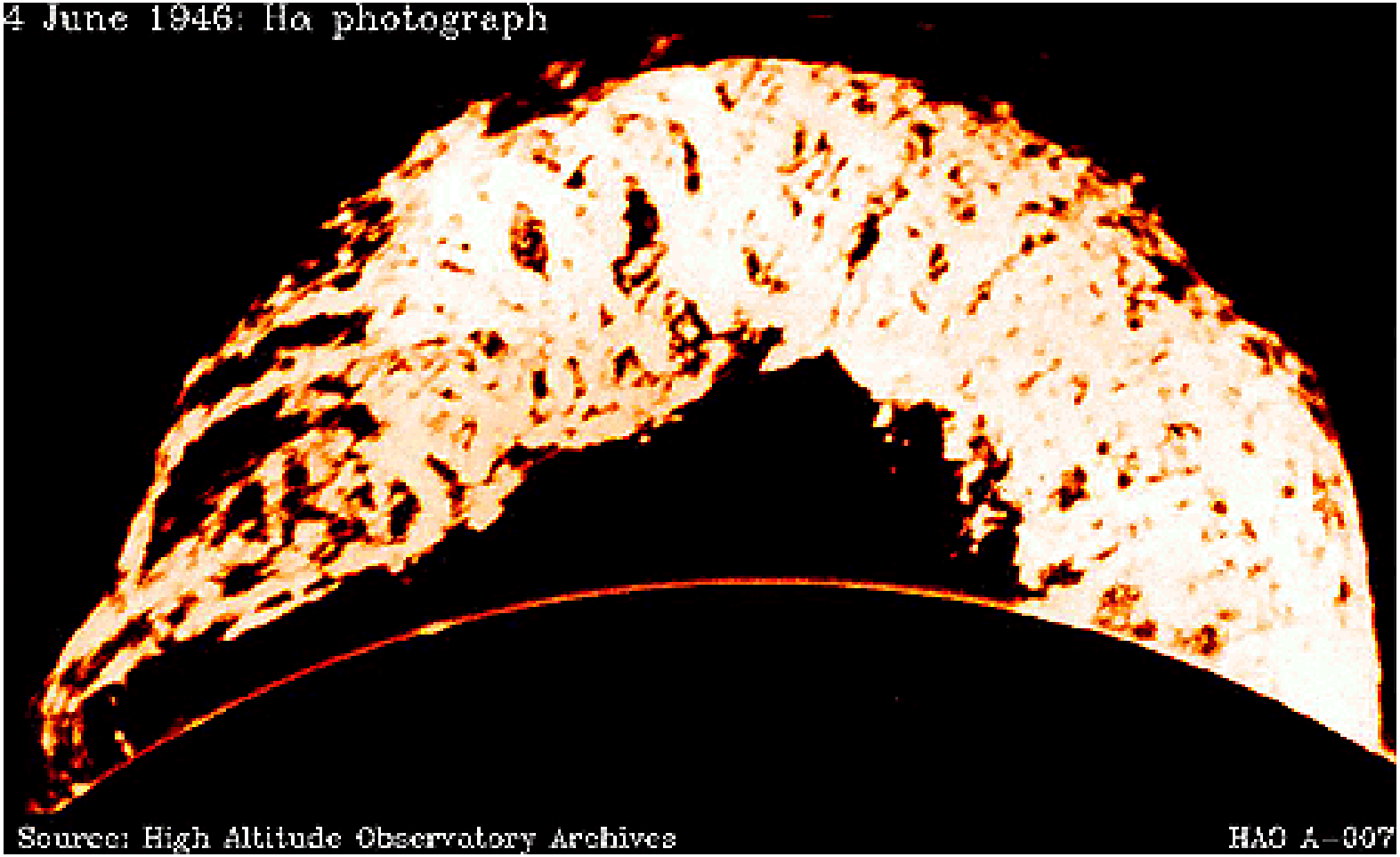

Modelo de erupción

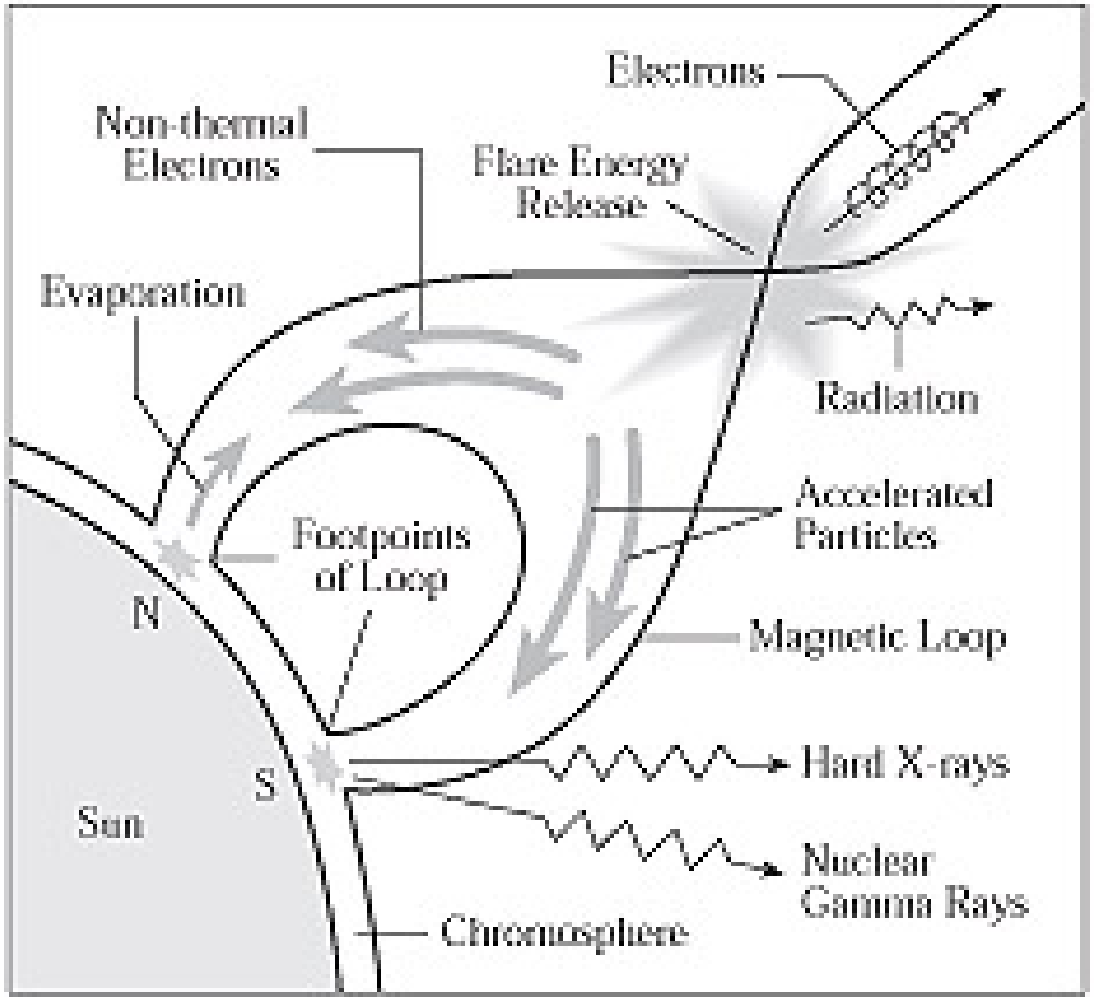

Corona solar

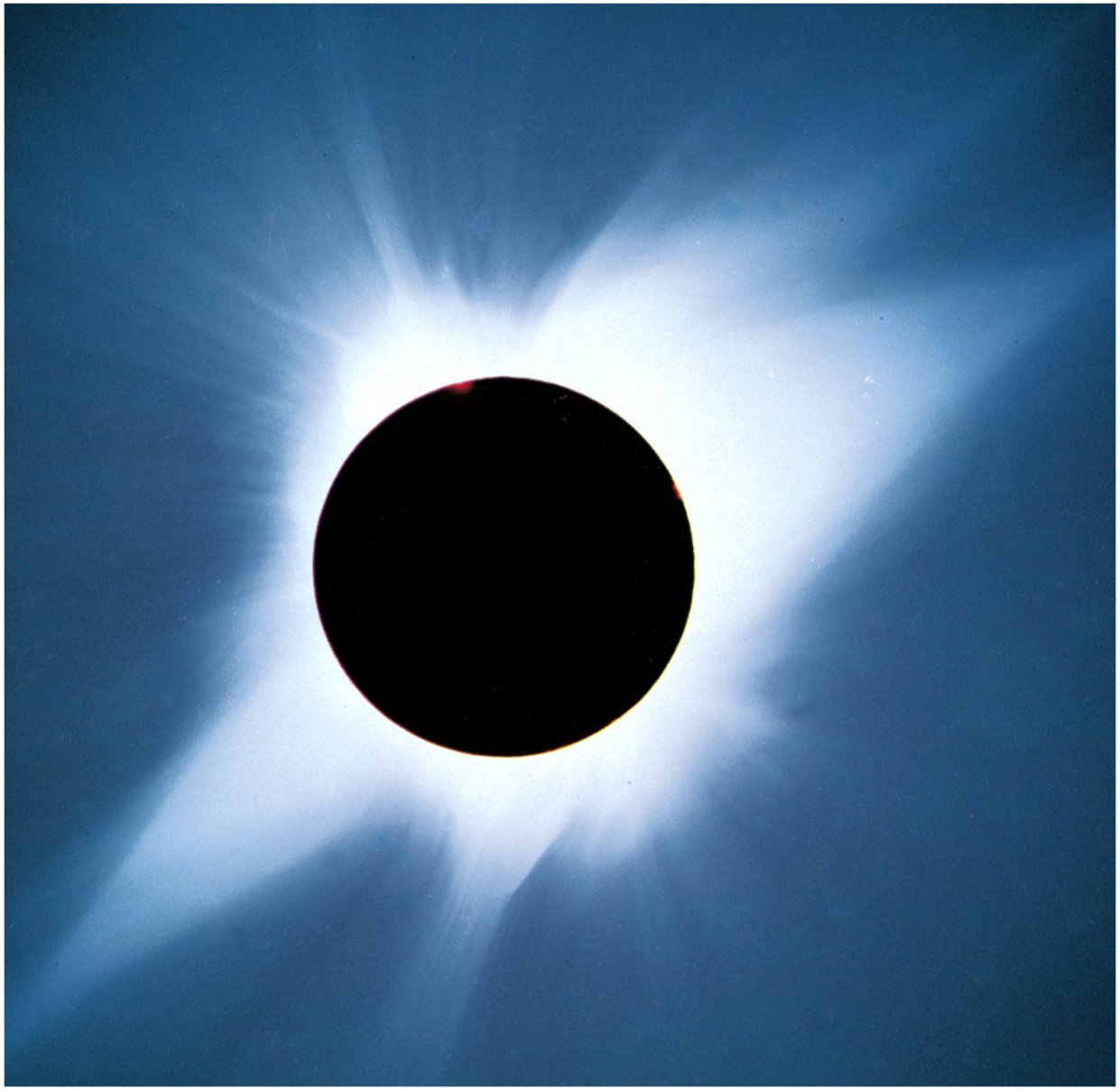

Interacción Sol-Tierra

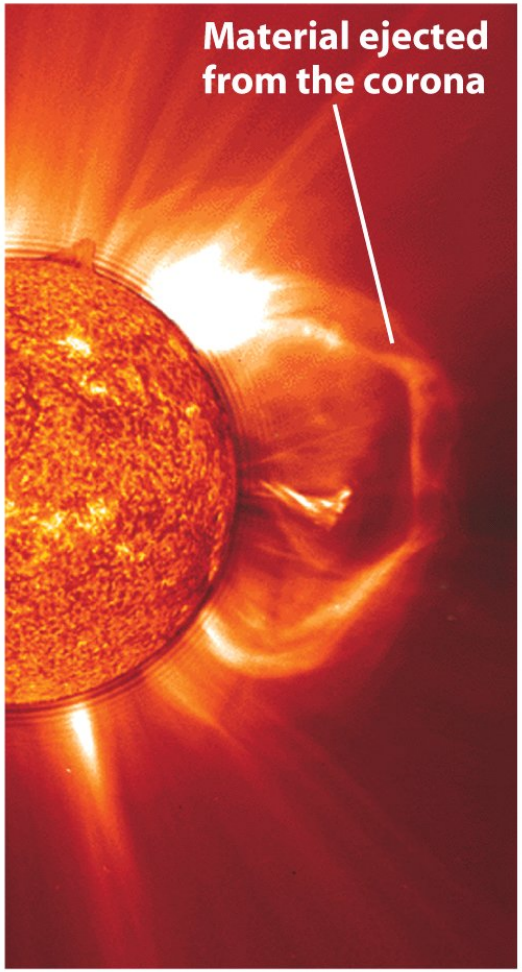

(a) A coronal mass ejection

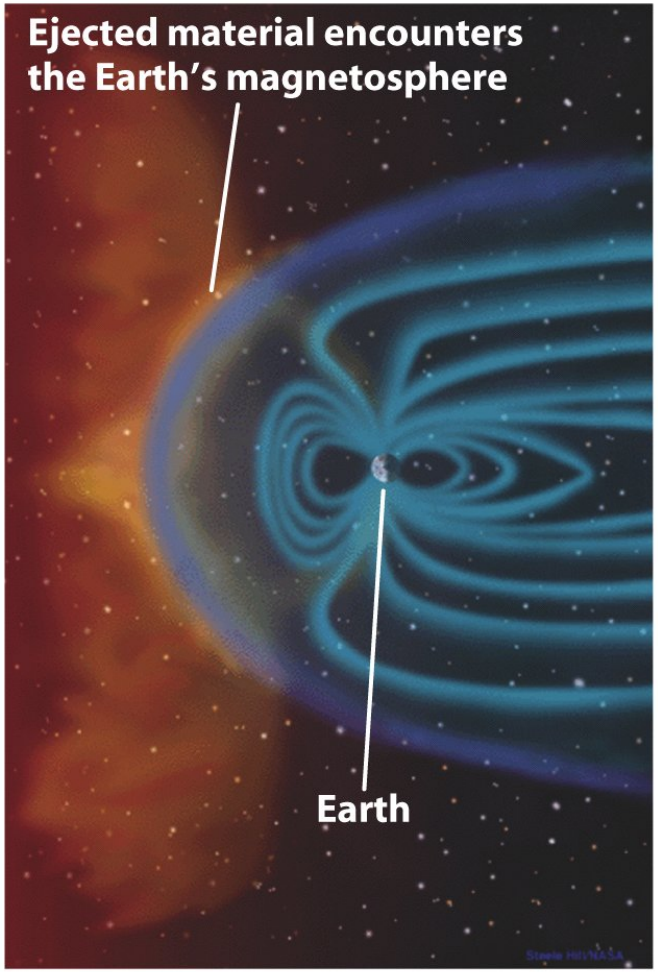

(b) Two to four days later

Aurora boreal

Erupción de rayos X

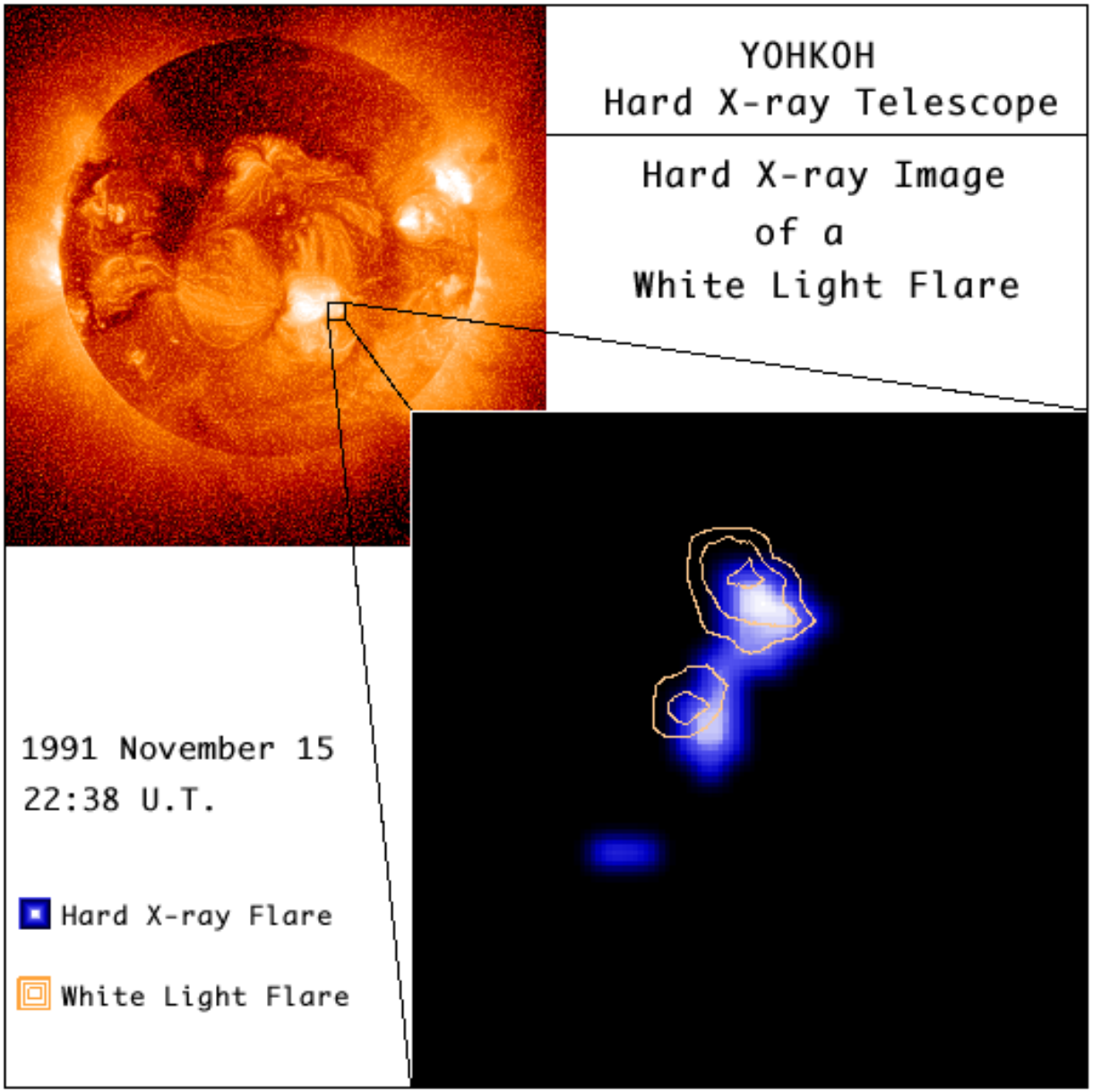

Erupción de rayos X

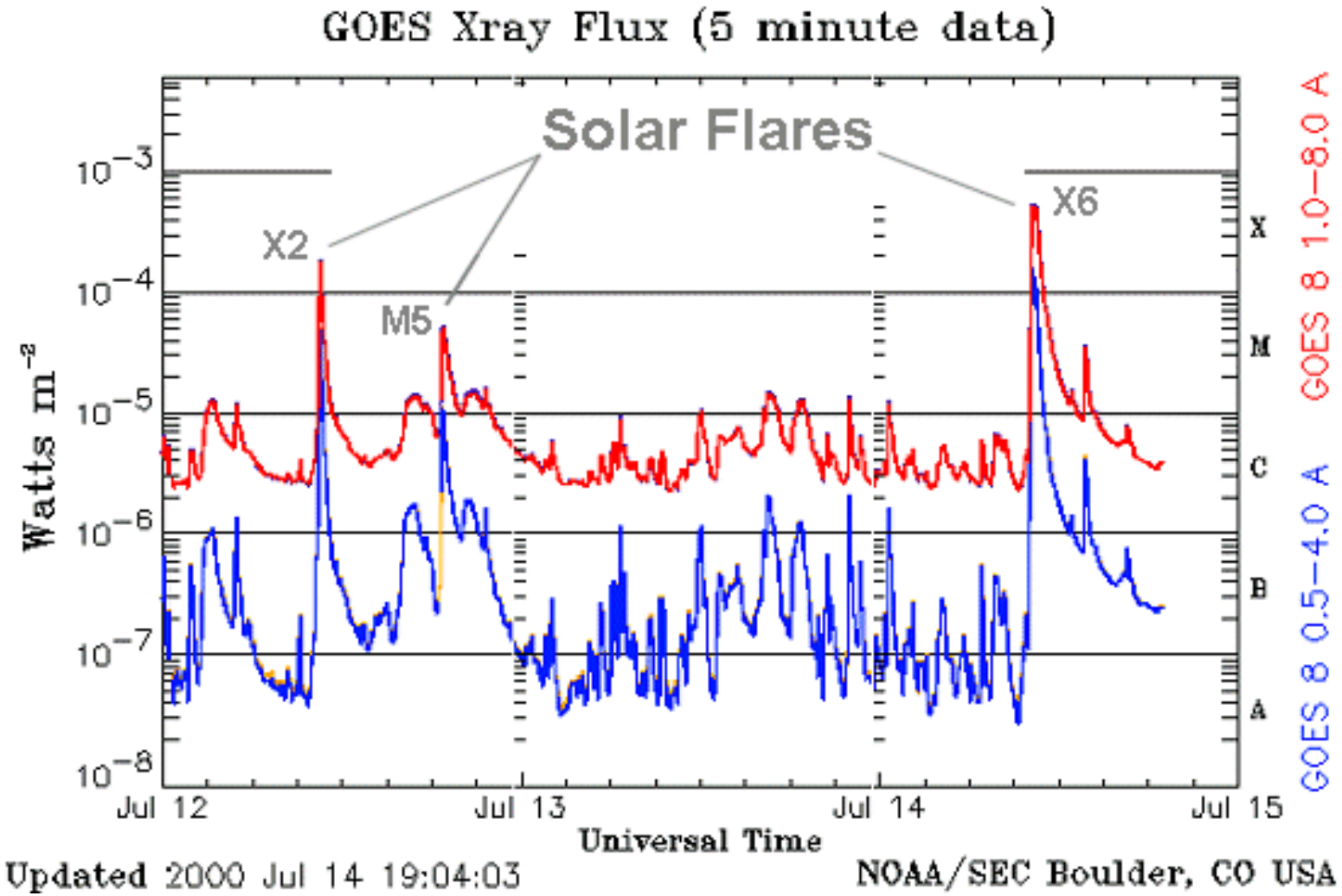

Erupción de rayos X

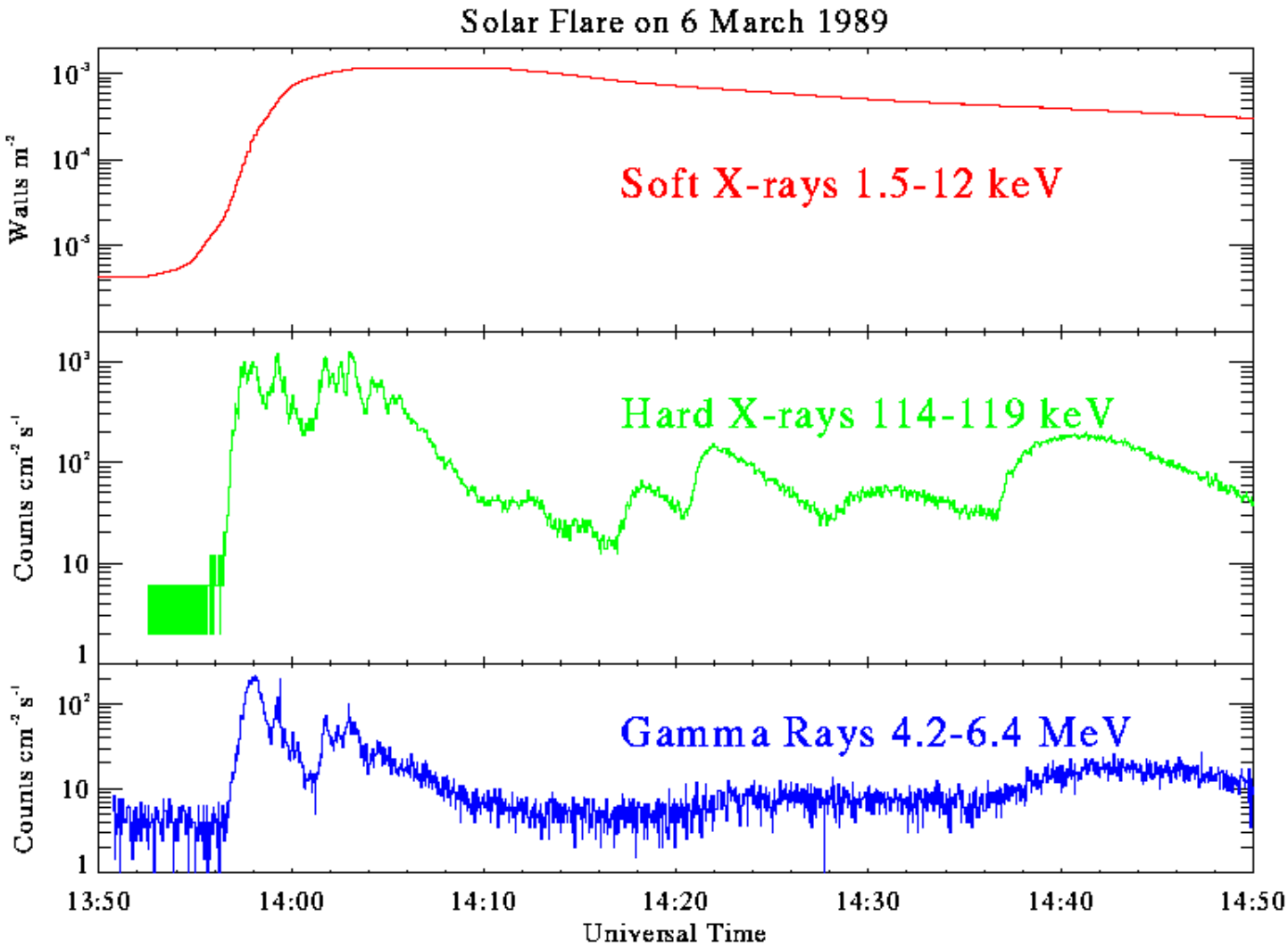

Erupción de rayos X

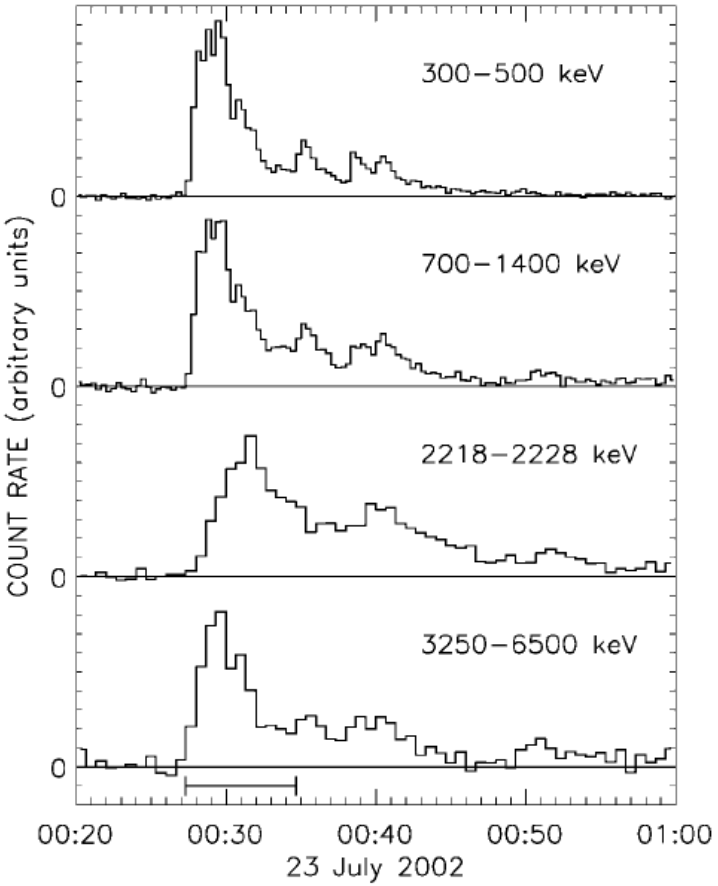

FIG. 1.—Background-subtracted light curves at the four imaged gamma-ray energy bands. Time resolutions are 20, 20, 40, and 40 s, respectively. The time interval used for mapping (00:27:20–00:34:40 UT) is shown at the bottom.

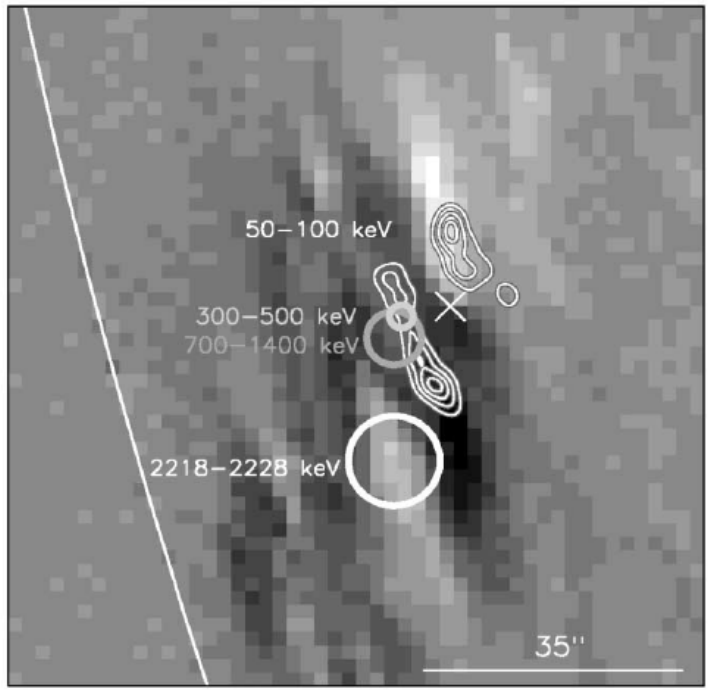

FIG. 4.—Locations of the gamma-ray sources. The thick circles represent the 1 σ errors for the 300–500 keV (*light gray*), 700–1400 keV (*dark gray*), and 2218–2228 keV (*white*) maps made with identical parameters. The 35″ FWHM angular resolution is shown in the lower right. The field of view is the same as in Fig. 3. The white contours show the high-resolution 50–100 keV map with 3″ resolution. The cross shows the centroid of the 50–100 keV emission made with the same lower resolution as the gamma-ray maps. The background image is a *SOHO*/MDI magnetogram acquired at 00:12 UT, 15 minutes prior to the flare.

Erupción de rayos X

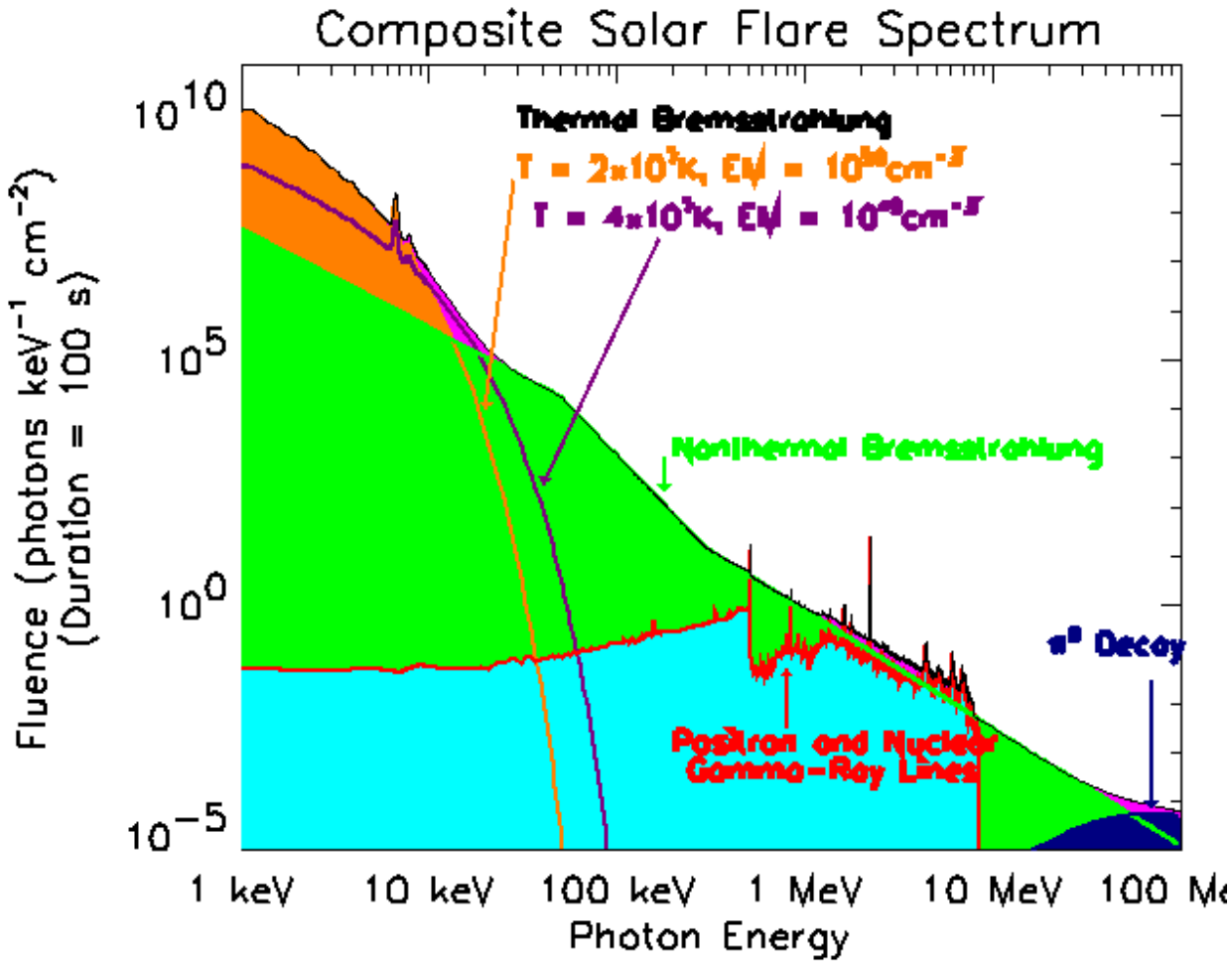

Líneas nucleares

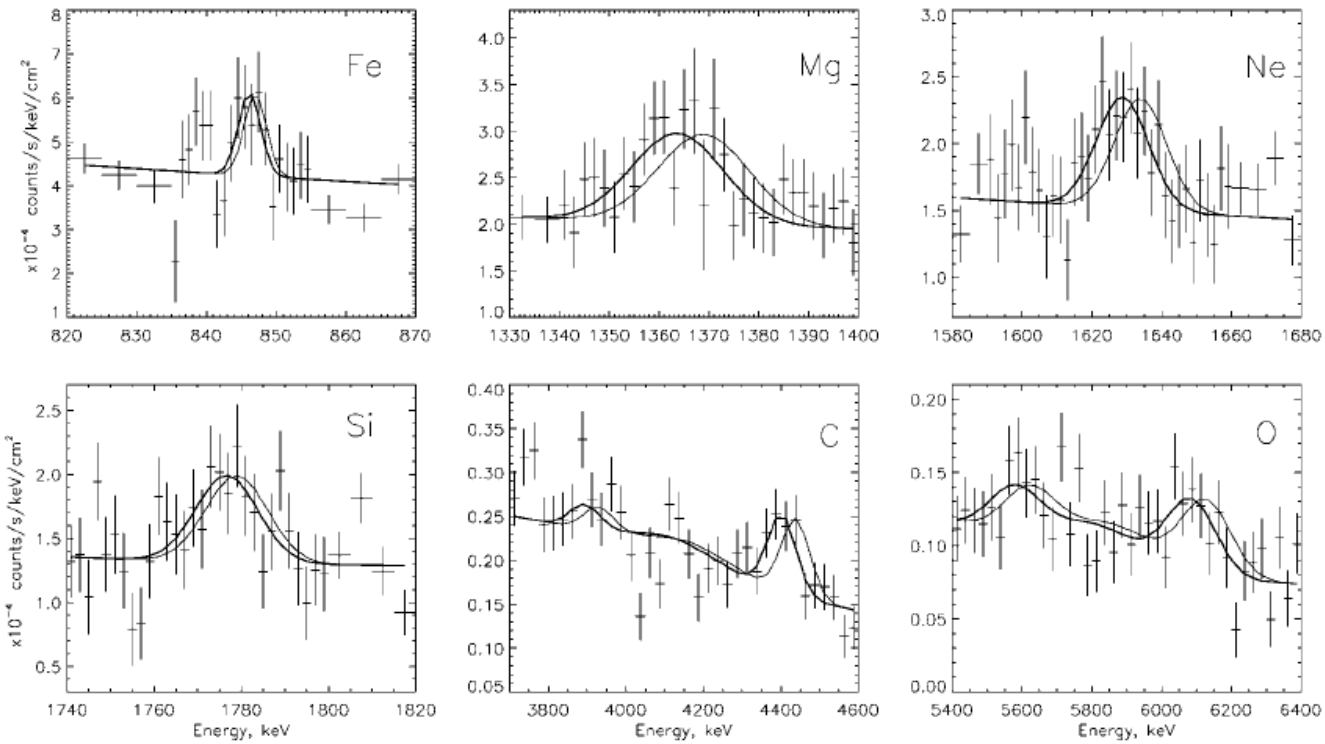

FIG. 1.—*RHESSI* background-subtracted count spectra from 00:27:20 to 00:43:20 UT on 2002 July 23. Each panel is labeled with the element primarily responsible for the line shown. The carbon and oxygen lines also show the secondary peak from the escape of a 511 keV positron-annihilation photon, which also contains information on the line shape. The thick curve shown in each panel is the Gaussian fit from Table 1 plus the underlying bremsstrahlung continuum and broad lines (see text), convolved with the instrument response. The thinner line is the same fit forced to zero redshift for comparison. The error bars are $\pm 1\ \sigma$ from Poisson statistics.

Estrellas activas

News December 2003: X-rays from the Pleiades

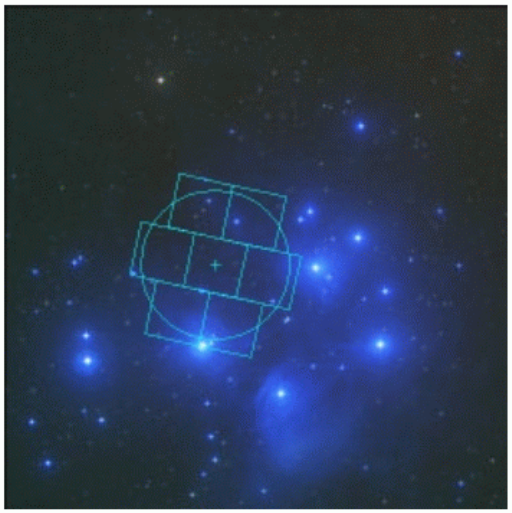

A large scale colour optical image of the Pleiades showing the region observed by XMM-Newton. The haziness of the bright stars is due to particles of dust in the cluster.

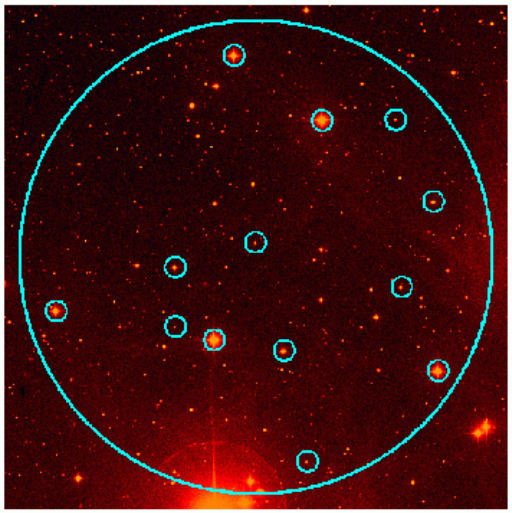

A smaller scale optical image (false colour) with the XMM-Newton survey region in detail, stars of spectral type A to K are circled.

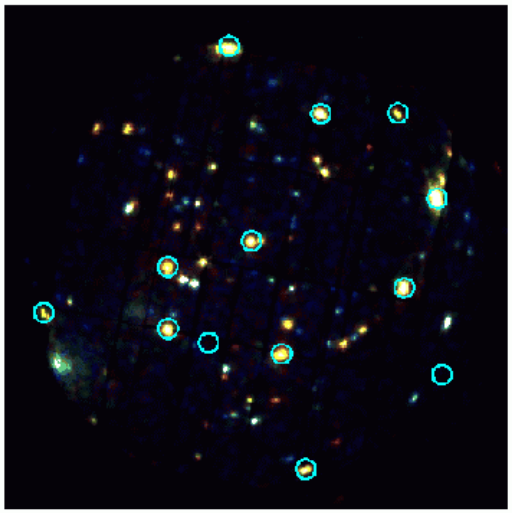

The XMM-Newton survey image showing the X-ray colours.

Estrellas activas

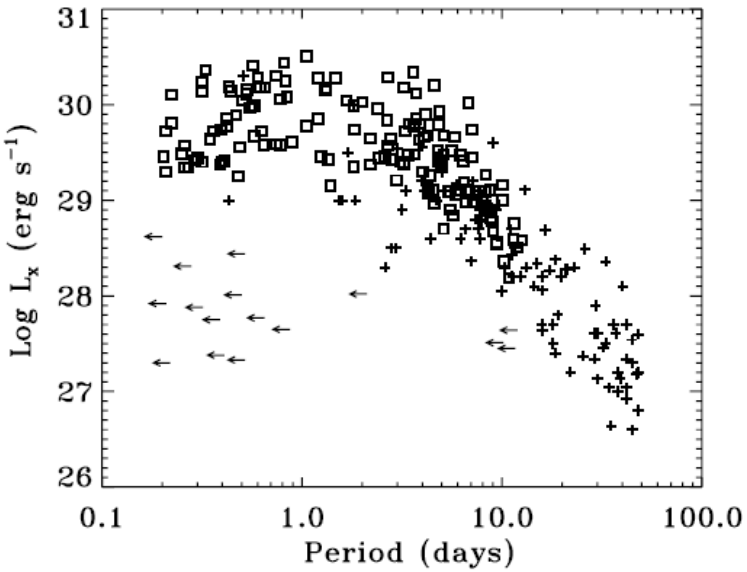

Fig. 3. X-ray luminosity vs. rotation period of field dwarfs (crosses) and cluster stars (squares). Leftward arrows indicate field stars with periods derived from $v \sin i$ data.

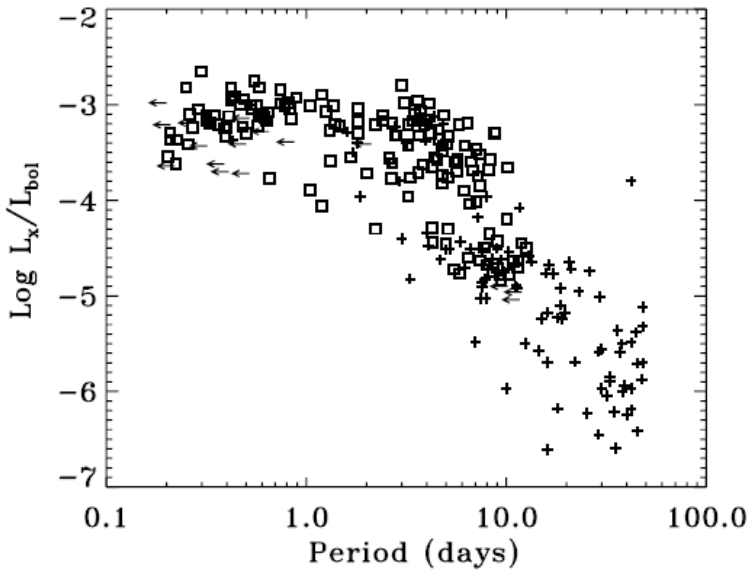

Fig. 4. X-ray to bolometric luminosity ratio vs. rotation period for field dwarfs (crosses) and cluster stars (squares). The meaning of the leftward symbols is the same as in Fig. 3.

Estrellas UV Cet

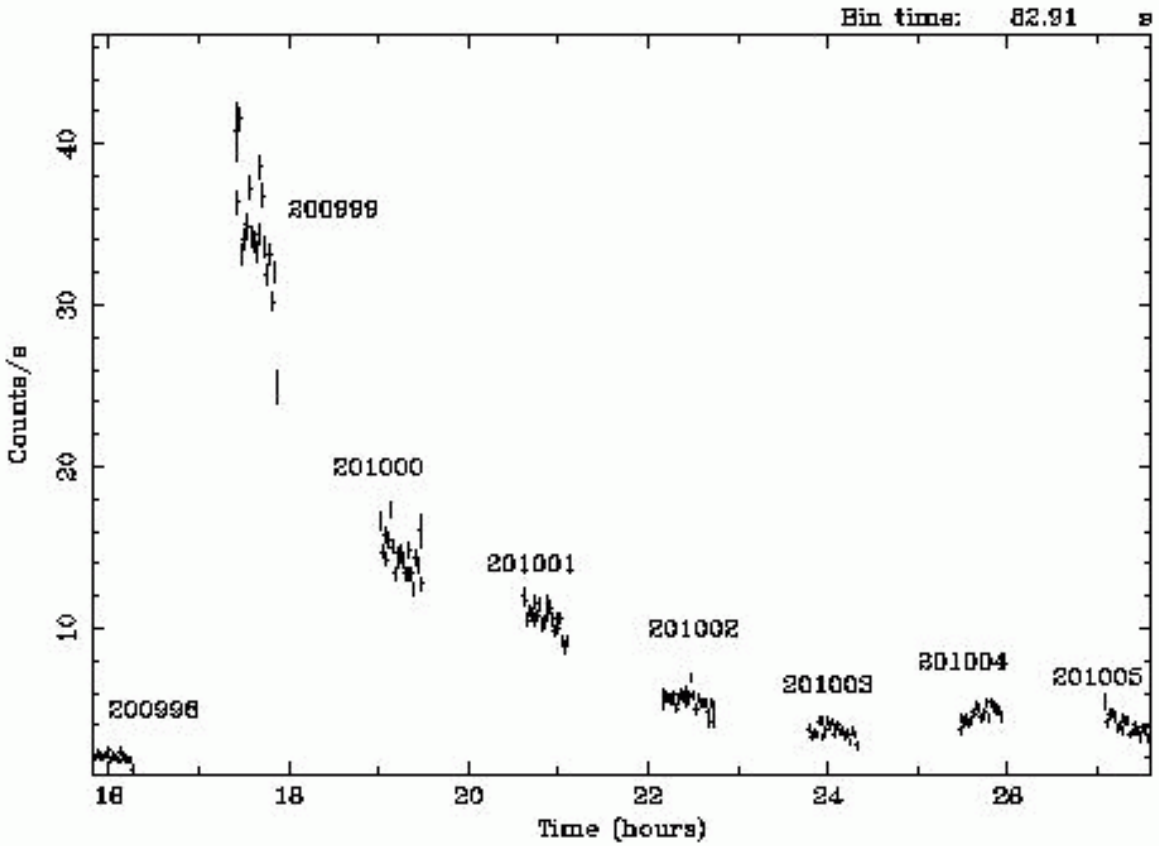

Figure 5.2: ROSAT light curve of the flare star GL355

Estrellas BY Dra y RS CVn

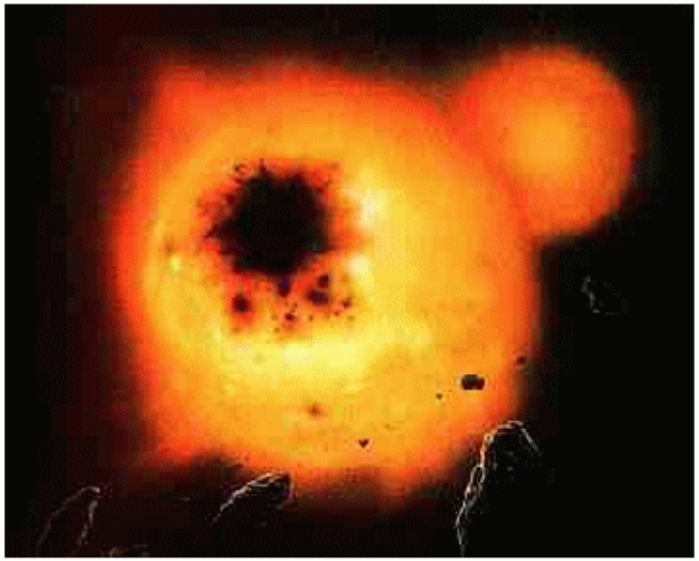

Representación artística de una RS Canum Venaticorum.

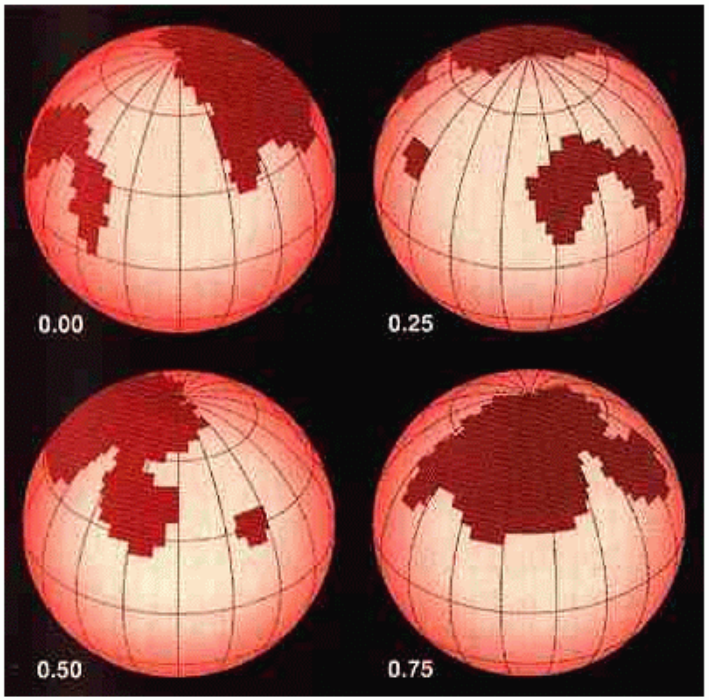

Modelo de una RS CVn realizado a partir de observaciones fotométricas. Se puede observar la superficie manchada en diversas fases del período y cómo el giro de la estrella es el responsable de las variaciones de luz.

Estrellas RS CVn

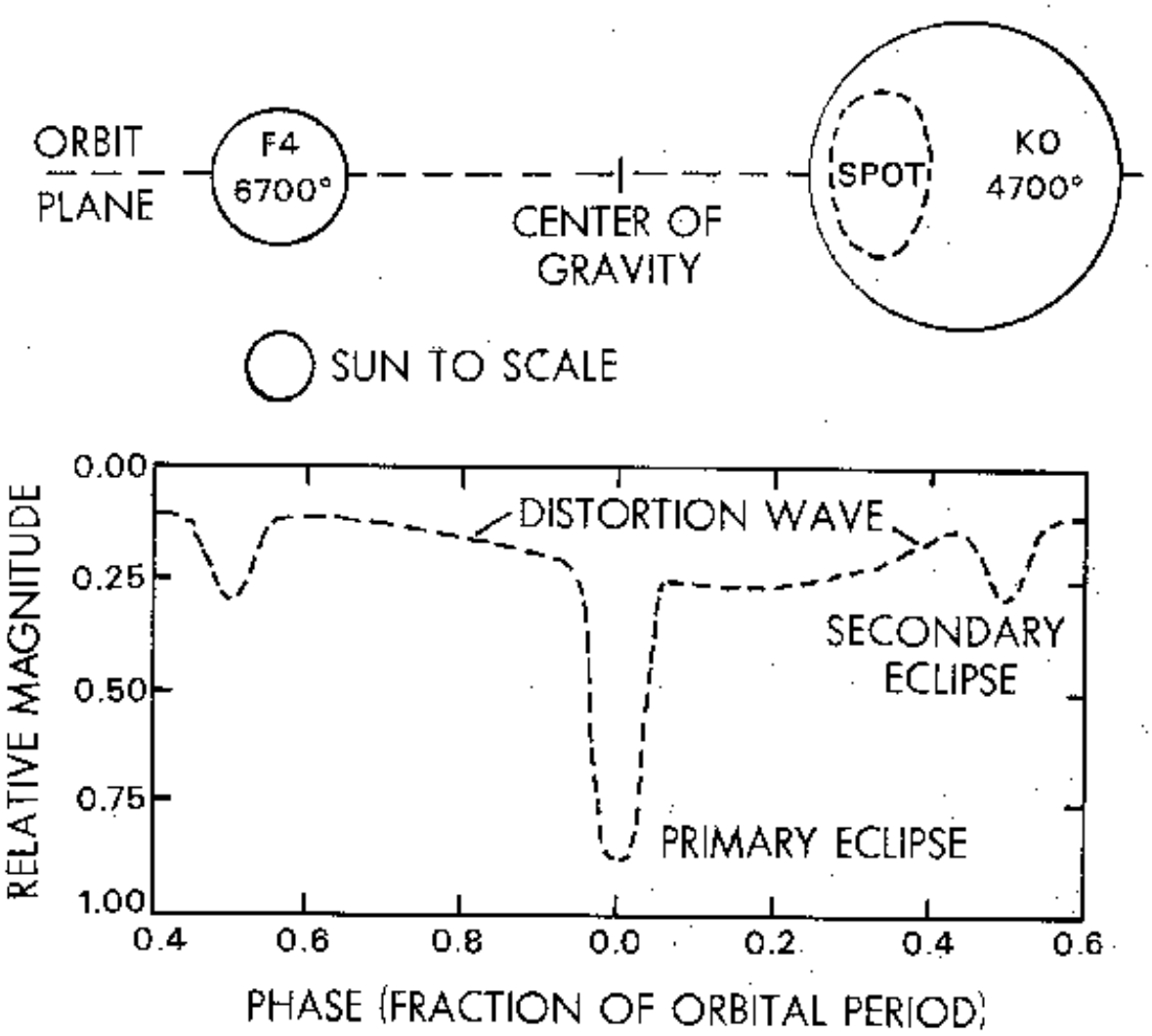

Estrellas BY Dra y RS CVn

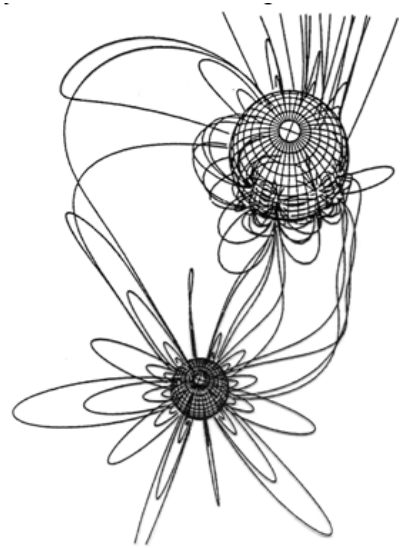

Left: Model of an RS CVn binary, showing interactions between stars due to their high field strengths and close proximity.

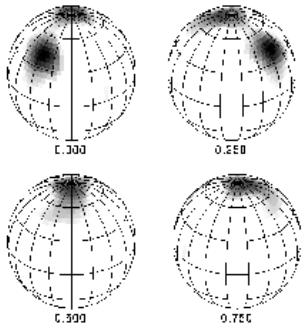

Right: Star spot mapping of the surface of one component of an RS CVn binary, showing that 10-20% of the stary may be covered with spots. The spot size and location is determined from eclipses and rotational modulation.

AD Leonis

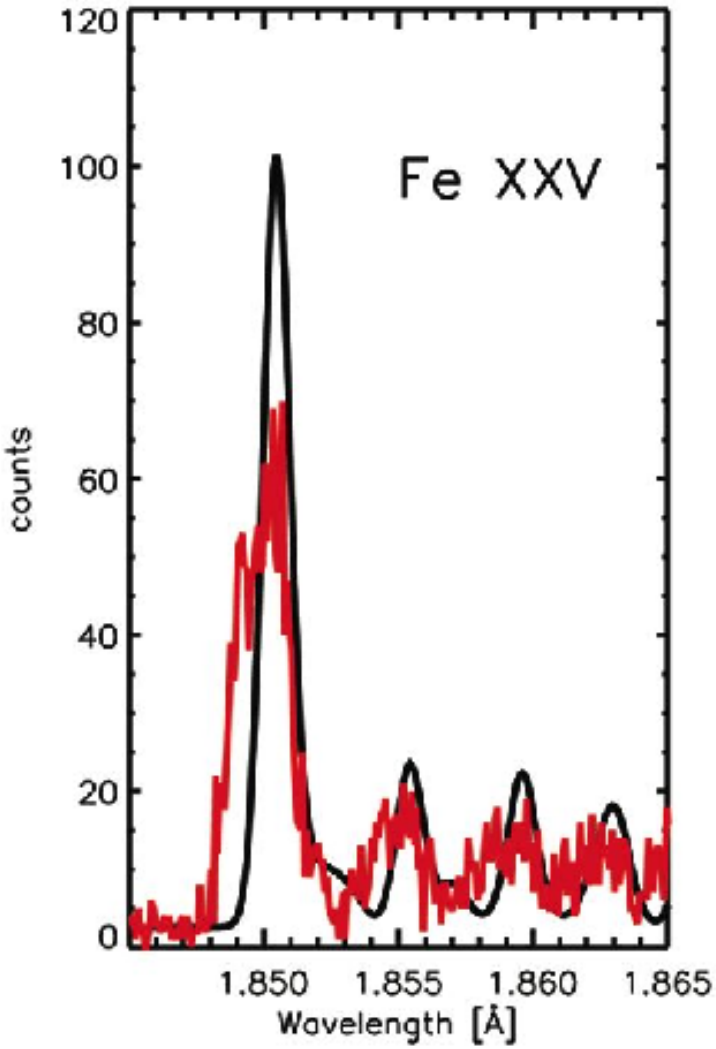
Fe XXV
counts
120
100
80
60
40
20
0
1.850
1.855
1.860
1.865
Wavelength [Å]

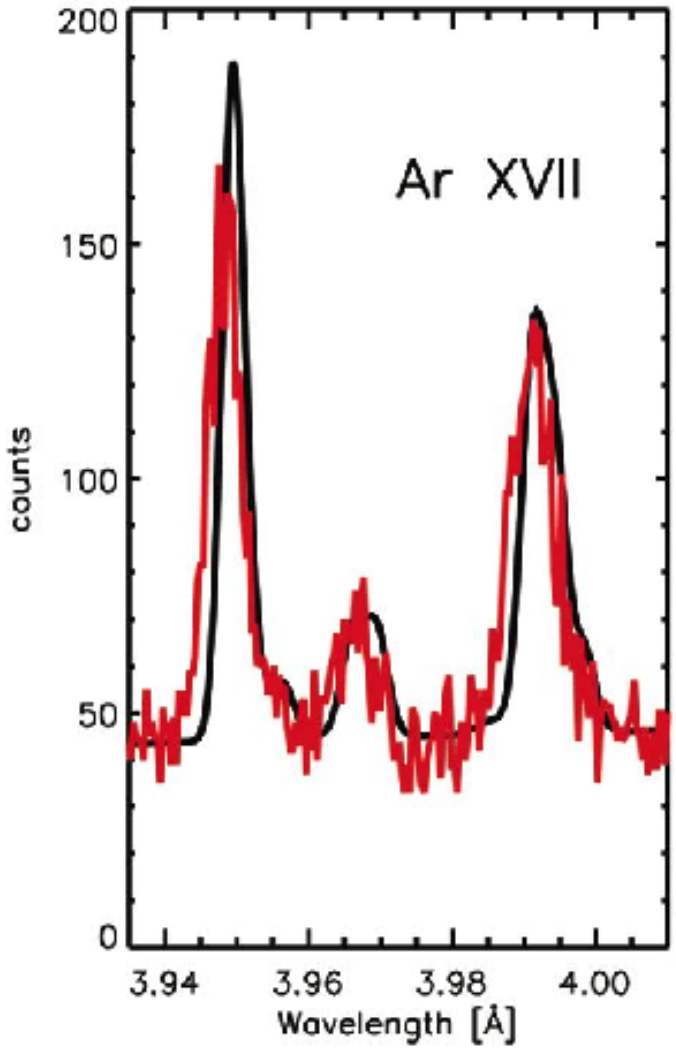
Ar XVII
counts
200
150
100
50
0
3.94
3.96
3.98
4.00
Wavelength [Å]

AR Lacertae

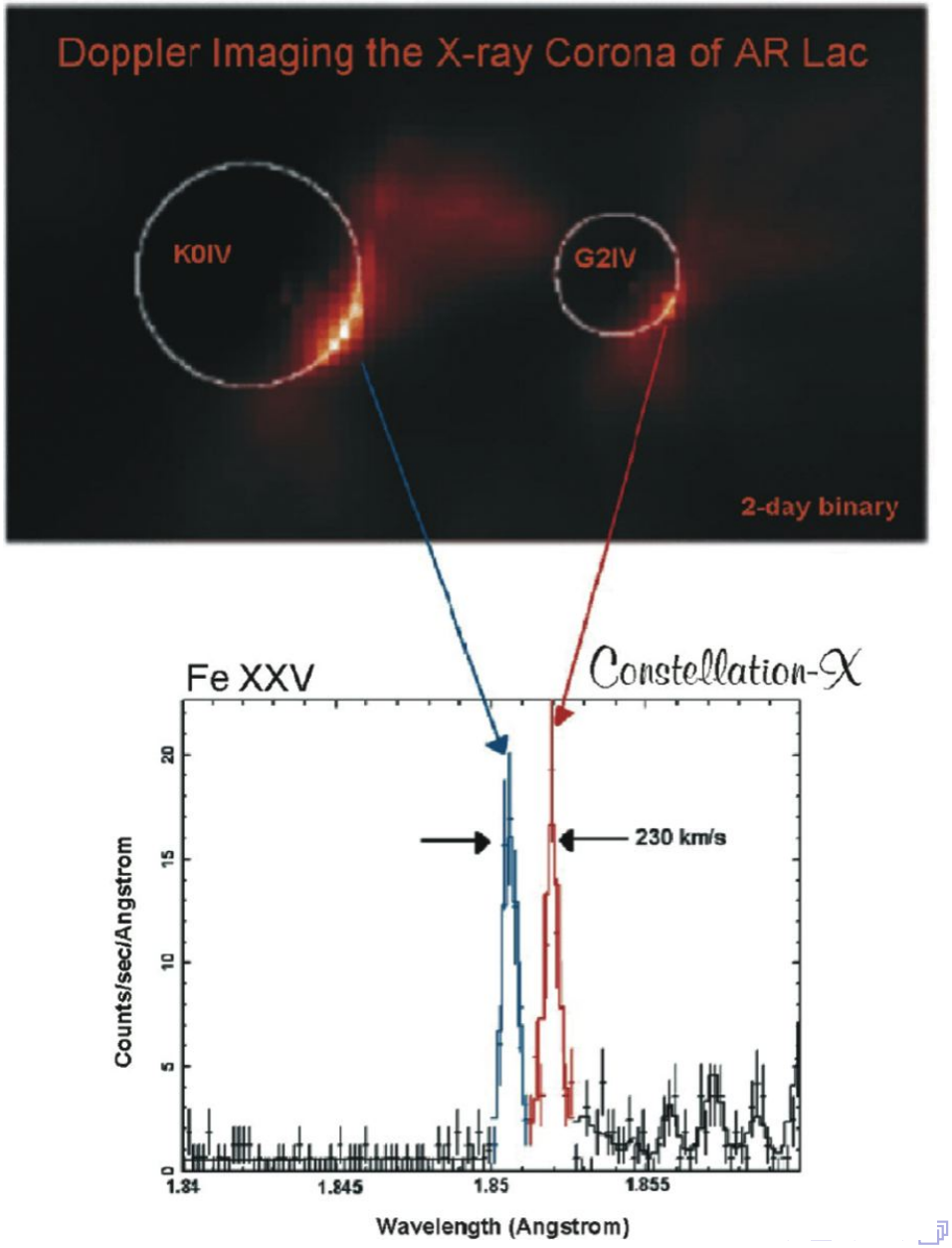
Doppler Imaging the X-ray Corona of AR Lac
K0IV
G2IV
2-day binary
Fe XXV
Constellation-X
230 km/s
Counts/sec/Angstrom
0
5
10
15
20
1.84
1.845
1.85
1.855
Wavelength (Angstrom)